

AD-A081 324

INSTITUTE FOR DEFENSE ANALYSES ARLINGTON VA SCIENCE A--ETC F/6 17/5
FIELD MANUAL TO DETERMINE DETECTION OR RECOGNITION RANGE OF A F--ETC(U)
SEP 79 L N SEEKAMP MDA-903-79-C-0202
IDA-P-1419 SBIE-AD-E500 112 NL

UNCLASSIFIED

| of |

AD
908-324



END
DATE
FORMED
4-80
DTIC

12 LEVEL II

IDA PAPER P-1419

FIELD MANUAL TO DETERMINE DETECTION
OR RECOGNITION RANGE OF A FLIR SENSOR

Lynne N. Seekamp

September 1979

DISTRIBUTION STATEMENT A

Approved for public release;
Distribution Unlimited

DTIC
ELECTE
MAR 5 1980
S D
B

REC FILE COPY AD A081324

Prepared for

Office of the Under Secretary of Defense for Research and Engineering

080 1 1 010



INSTITUTE FOR DEFENSE ANALYSES
SCIENCE AND TECHNOLOGY DIVISION

The work reported in this document was conducted under contract MDA 903 79 C 0202 for the Department of Defense. The publication of this IDA Paper does not indicate endorsement by the Department of Defense, nor should the contents be construed as reflecting the official position of that agency.

Approved for public release; distribution unlimited.

UNCLASSIFIED

SECURITY CLASSIFICATION OF THIS PAGE (When Data Entered)

REPORT DOCUMENTATION PAGE		READ INSTRUCTIONS BEFORE COMPLETING FORM
1. REPORT NUMBER	2. GOVT ACCESSION NO.	3. RECIPIENT'S CATALOG NUMBER
4. TITLE (and Subtitle) <u>FIELD MANUAL TO DETERMINE DETECTION OR RECOGNITION RANGE OF A FLIR SENSOR</u>		5. TYPE OF REPORT & PERIOD COVERED <u>FINAL rept's</u>
7. AUTHOR(s) <u>Lynne N. Seekamp</u>		6. PERFORMING ORG. REPORT NUMBER <u>IDA PAPER P-1419</u>
9. PERFORMING ORGANIZATION NAME AND ADDRESS <u>INSTITUTE FOR DEFENSE ANALYSES 400 Army-Navy Drive Arlington, Virginia 22202</u>		8. CONTRACT OR GRANT NUMBER(s) <u>MDA-903-79-C-0202</u>
11. CONTROLLING OFFICE NAME AND ADDRESS <u>DUSD (Research and Advanced Technology) The Pentagon, Washington, D.C. 20301</u>		10. PROGRAM ELEMENT PROJECT TASK AREA & WORK UNIT NUMBERS <u>Task T-136</u>
14. MONITORING AGENCY NAME & ADDRESS (if different from Controlling Office) <u>Defense Advanced Research Projects Agency 1400 Wilson Boulevard Arlington, Virginia 22209</u>		12. REPORT DATE <u>Sep 1979</u>
		13. NUMBER OF PAGES <u>28</u>
16. DISTRIBUTION STATEMENT (of this Report) <u>Approved for public release; distribution unlimited.</u>		15. SECURITY CLASS. (of this report) <u>UNCLASSIFIED</u>
		15a. DECLASSIFICATION DOWNGRADING SCHEDULE <u>N/A</u>
17. DISTRIBUTION STATEMENT (of the abstract entered in Block 20, if different from Report) <u>None</u>		14. <u>IDA-P-1419</u>
18. SUPPLEMENTARY NOTES <u>N/A</u>		DTIC ELECTE S D MAR 5 1980
19. KEY WORDS (Continue on reverse side if necessary and identify by block number) <u>forward-looking infrared systems, atmospheres, transmittance, aerosols, attenuation, signal-to-noise ratio, detection, recognition, range (distance)</u>		B
20. ABSTRACT (Continue on reverse side if necessary and identify by block number) <u>Forward-looking infrared (FLIR) sensor performance range estimates over a horizontal path can be made by using a rapid estimation procedure. These estimates can be calculated while in the field by using a hand calculator for several different FLIR systems, atmospheric transmission conditions, and levels of difficulty of the visual task.</u>		

DD FORM 1473 1 JAN 73 EDITION OF 1 NOV 65 IS OBSOLETE

UNCLASSIFIED

SECURITY CLASSIFICATION OF THIS PAGE (When Data Entered)

403108 204

IDA PAPER P-1419

FIELD MANUAL TO DETERMINE DETECTION
OR RECOGNITION RANGE OF A FLIR SENSOR

Lynne N. Seekamp

September 1979



INSTITUTE FOR DEFENSE ANALYSES
SCIENCE AND TECHNOLOGY DIVISION
400 Army-Navy Drive, Arlington, Virginia 22202

Contract MDA 903 79 C 0202
Task T-136

ACKNOWLEDGMENTS

The methodology for the rapid calculation procedure to predict FLIR performance discussed in this paper was developed by Dr. Robert E. Roberts of the Institute for Defense Analyses. The author thanks R.E. Roberts, L.M. Biberman and M.L. Sullivan of the Institute for Defense Analyses for their useful discussions and contributions to this paper.

RE: Classified references, distribution unlimited-
Delete classified references per Mr. Walter Hanley, IDA/Security

ACCESSION for	
NTIS	White Section <input checked="" type="checkbox"/>
DDC	Buff Section <input type="checkbox"/>
UNANNOUNCED	<input type="checkbox"/>
JUSTIFICATION _____	
BY _____	
DISTRIBUTION/AVAILABILITY CODES	
Dist.	AVAIL and/or SPECIAL
A	

CONTENTS

Acknowledgments	11
I. INTRODUCTION	1
II. METHODOLOGY	3
III. INPUT DATA	11
A. FLIR System Specifications	12
B. Task Level Factors	13
C. Target Specifications	15
D. Atmospheric Factors	16
IV. AN EXAMPLE OF THE CALCULATION PROCEDURE	22
References	25

I. INTRODUCTION

This publication is designed to be a concise manual for assessing forward-looking infrared (FLIR) sensor performance ranges under a variety of conditions and thus is directed toward the operator in the field. The purpose of this publication is to present a summary of the methodology used to derive the FLIR performance rapid estimation procedure, present tables of input values for several different FLIR systems, atmospheric transmission conditions and levels of difficulty of the visual task, and show an example of the calculation procedure. In this paper we will use what we believe are the best data bases and models currently available. However, uncertainties still exist regarding some of these data, particularly with respect to the prediction of aerosol extinction. These uncertainties will be discussed in the appropriate sections.

A previous publication described a computer code developed to model the performance of a FLIR sensor (Ref. 1). The computer code (Program FLIR) was used to calculate the probabilities of detection and recognition of a target by an observer using a FLIR sensor. Since that time a rapid approximation for calculating the range at various probabilities of detection or recognition for a given FLIR system has been developed. We felt that it would be useful to publish a concise manual that could be used in the field as a guide for making quick estimates of FLIR performance. It should be noted that the procedure outlined here is applicable only to estimating FLIR performance over horizontal paths. The equation used to estimate FLIR performance was derived by R.E. Roberts of the Institute for Defense Analyses (Refs. 2, 3).

The calculation method presented here is designed to be used with a hand calculator when a fast determination of range at various probabilities of detection or recognition is required.

II. METHODOLOGY

An equation has been derived which directly shows the range at 50 percent probability (as well as at other probabilities) as a function of target, system, environment, and task parameters. An explanation of the derivation of this equation and the validation are given in IDA Paper P-1284, *A Simplified Approach to Analyses of Infrared Sensor Performance Versus Weather: Theory and Application to the Hannover Data Base (U)* (Ref. 2). A brief discussion of the methodology will be reviewed below.

The most common parameter used to characterize FLIR performance is the minimum resolvable temperature (MRT). Usually this represents a plot of the values of minimum resolvable temperature difference between a pattern of four identical bars and the three spaces between them for each of a number of spatial frequencies. The bars represent a blackbody source of temperature $T + \Delta T$, where T is the background temperature (in degrees Kelvin) and ΔT is the difference between the background temperature and the target temperature. The spaces represent the background temperature T . MRT then is the minimum ΔT that a standard observer can resolve through a given FLIR. The four bars and three equal-sized spaces form a square, and thus the aspect (length:width) ratio of each bar and space is 7:1 (Fig. 1).

J. Johnson has shown that many objects may be represented by pairs of black and white bars inside a square (Ref. 4). He related the number of line pairs of a bar chart, where the pairs fit inside the minor dimension of an object, with the ability of an observer to detect (resolve one pair of bars) or recognize (resolve four pairs of bars) the object. The task level

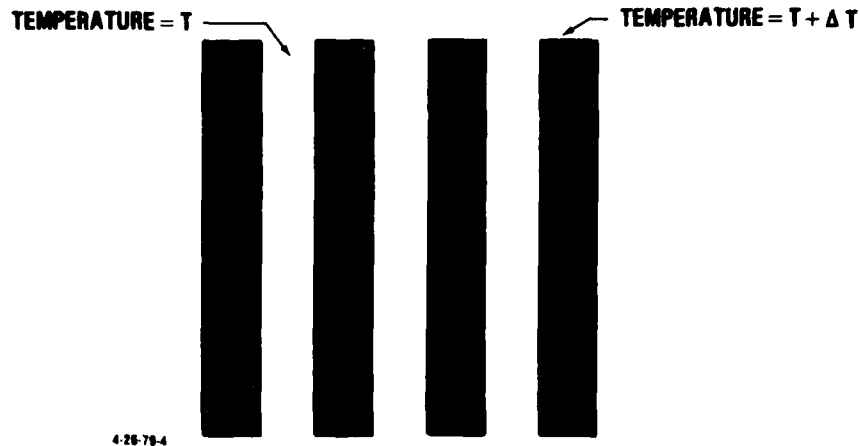


FIGURE 1. Standard four-bar MRT test pattern.

factor γ is the number of line pairs; for example, for detection $\gamma = 1$ and for recognition $\gamma = 4$. Johnson's conclusion was based on the assumption that the object or target and the equivalent bar pattern were of the same size and contrast and at the same distance.

F.A. Rosell introduced the concept of aspect corrections for targets whose shapes are significantly different from the square used in the standard equivalent bar patterns (Ref. 5). As a result, the laboratory-measured value of MRT using the standard four-bar square test pattern with an aspect ratio of 7:1 is divided by $\sqrt{\epsilon/7}$ in order to obtain an aspect-corrected value of MRT. The letter ϵ is the length-to-width ratio of a single resolution bar in the pattern which represents the actual target rectangular outline. Figure 2 shows an automobile with major dimension (length) approximately twice the minor dimension (height) and the corresponding bar patterns for detection and recognition. In this figure the aspect ratio of a single bar for detection is 4:1 and that for recognition is 16:1.

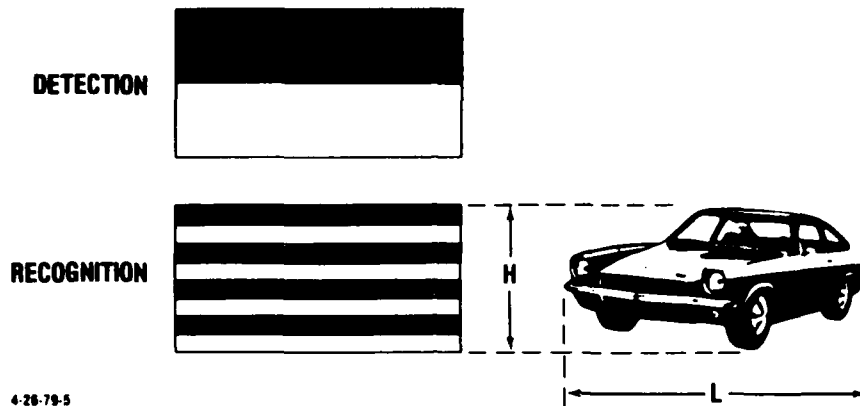


FIGURE 2. Object image and corresponding bar patterns for detection and recognition.

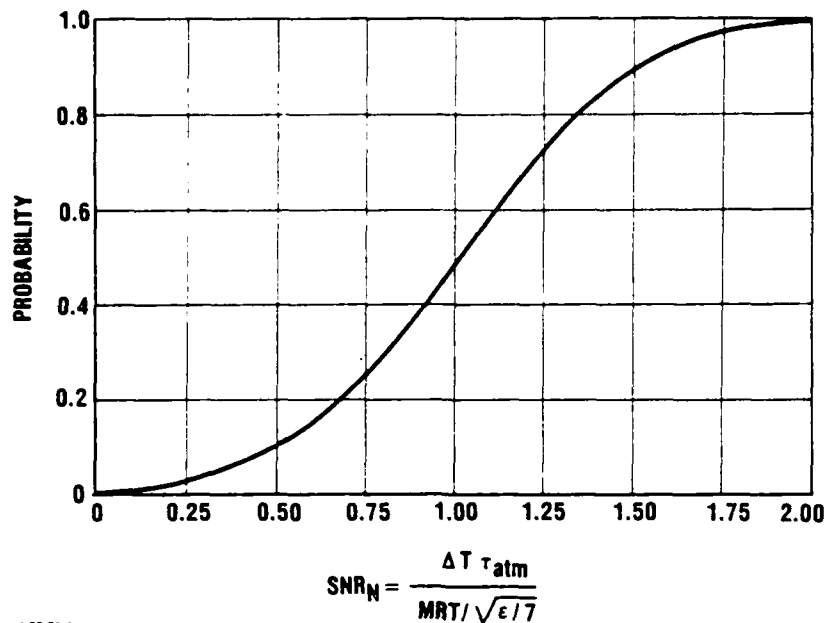
The temperature difference between a target and its background is represented by ΔT (in degrees Kelvin). However, at a distance the apparent temperature differential between the target and the background will be less because of atmospheric attenuation of the target radiation. The atmospherically degraded thermal contrast is obtained by multiplying ΔT by the atmospheric transmission τ_{atm} .

The ratio of the atmospherically degraded thermal contrast to the aspect-corrected value of MRT is a normalized signal-to-noise ratio (SNR). Thus, the normalized SNR is given by the expression:

$$SNR_N = \frac{\Delta T \tau_{atm}}{MRT/\sqrt{\epsilon/\gamma}} \quad (1)$$

Equation 1 is the fundamental expression used in FLIR performance modeling.

It has been shown that the probability of carrying out a given task of detection or recognition is related to the normalized SNR as indicated in Fig. 3. These data were generated



4-28-79-4

FIGURE 3. Probability of detection or recognition versus normalized signal-to-noise ratio.

theoretically and from a series of experiments using many observers (Ref. 6). The SNR is normalized in such a way that when $SNR_N = 1.0$ the probability of achieving the task (detection or recognition) is 50 percent. Other values of SNR_N will yield different probabilities of achieving the task (Fig. 3).

The solution to Eq. 1 for performance range is greatly simplified by making the following assumptions.

First, atmospheric transmission often may be approximated by Beer's law for narrow spectral intervals or spectral regions where there is a relatively weak range dependence such as for the water vapor continuum or aerosol extinction. If we assume a Beer's law dependence, we obtain

$$\tau_{atm} = e^{-\delta_{atm} R} \quad , \quad (2)$$

where β_{atm} is the extinction coefficient of the atmosphere and R is range (usually in kilometers). The coefficient β_{atm} is the sum of the extinction coefficients due to molecular absorption, water vapor continuum, and aerosols:

$$\beta_{\text{atm}} = \beta_{\text{mol}} + \beta_{\text{H}_2\text{O cont}} + \beta_{\text{aer}} .$$

Look-up tables of $\beta_{\text{mol}} + \beta_{\text{H}_2\text{O cont}}$ are presented later. It is evident from these tables of extinction coefficients for different path lengths that β_{mol} has a weak dependence on range. The example provided will show how to deal with this problem in a practical way. The dominant causes of atmospheric attenuation, namely aerosols and the water vapor continuum, are relatively independent of range.

We next assume that the system MRT also can be adequately approximated by an exponential function:

$$\text{MRT} = \text{MRT}_0 e^{\beta_{\text{sys}} v} . \quad (3)$$

Figure 4 shows MRT_0 , β_{sys} , and v on a plot of the logarithm of minimum resolvable temperature (MRT) versus spatial frequency in cycles/milliradian, where MRT_0 is the y-intercept of the regression line, β_{sys} is the system extinction coefficient, and v is the spatial frequency in cycles/milliradian. If the size (S) of the target (the minor dimension in meters) and the task level factor (γ) defined according to the Johnson equivalent-bar-pattern criteria are known, then we have

$$v = \frac{\gamma}{S} R .$$

This equation provides a scaling factor for the abscissa in Fig. 4.

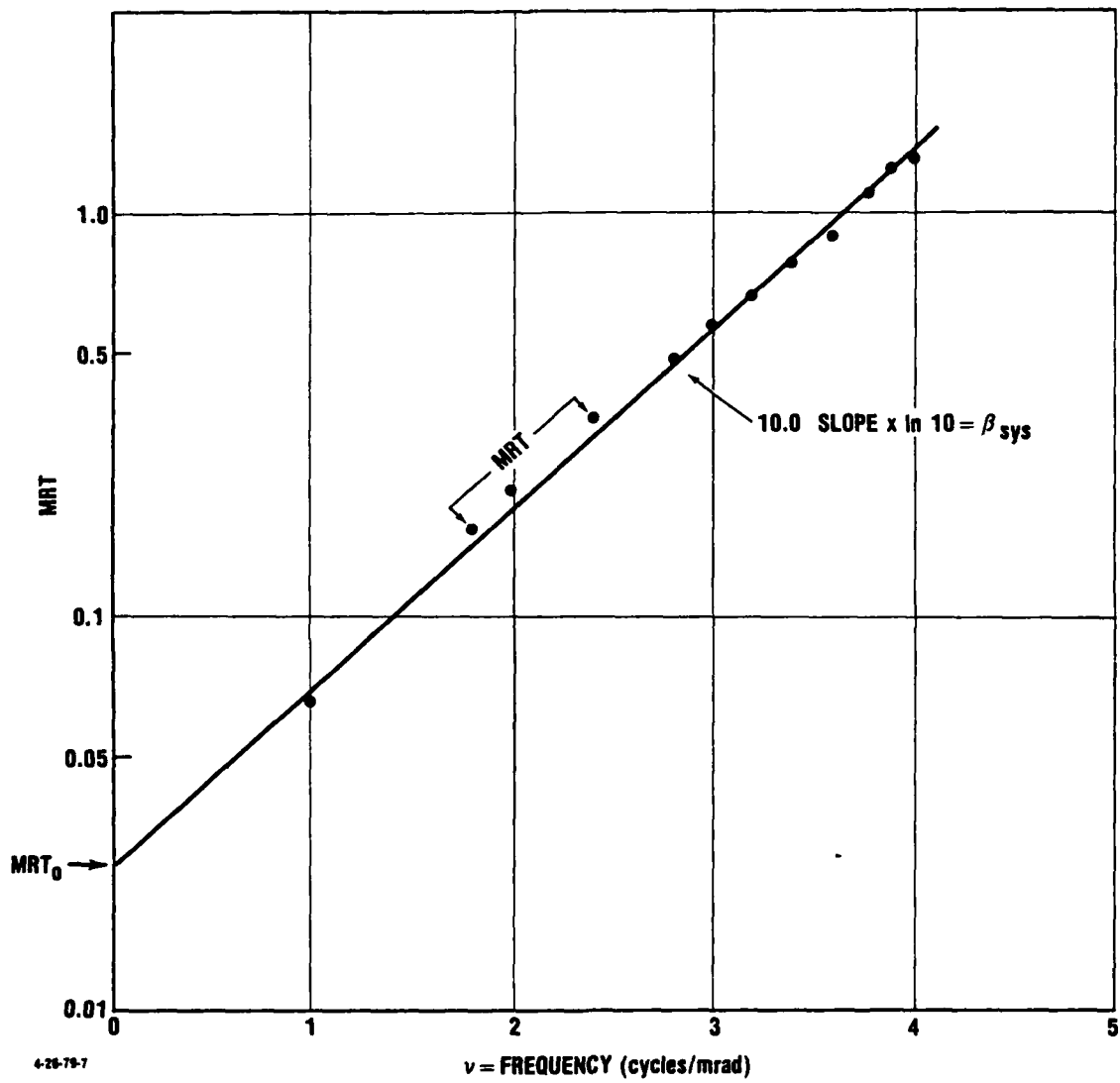


FIGURE 4. Sample MRT.

Substituting $\frac{Y}{S} R$ for v in Eq. 3 yields

$$MRT = MRT_0 e^{\frac{Y}{S} \beta_{sys} R} \quad (4)$$

The performance range in kilometers at the 50 percent confidence level is then obtained by substituting Eqs. 2 and 4 into Eq. 1 for β_{atm} and MRT, respectively, and by setting $SNR_N = 1$, which by definition gives a probability of 50 percent of achieving the task (Fig. 3):

$$1 = \frac{\Delta T e^{-\beta_{atm} R}}{MRT_0 e^{\frac{Y}{S} \beta_{sys} R} / \sqrt{\epsilon/\eta}} \quad (5)$$

Equation 5 is then solved for R:

$$R = \frac{\ln \frac{\Delta T \sqrt{\epsilon/\eta}}{MRT_0}}{\beta_{atm} + \frac{Y}{S} \beta_{sys}} \quad (6)$$

Table 1 shows values of MRT_0 and β_{sys} for two FLIR systems representing 1974 and 1978-79 technology devices. The coefficient of determination r^2 is based on a regression on Eq. 3 and is an indication that the two parameters MRT_0 and β_{sys} are valid descriptors of MRT.

TABLE 1. REPRESENTATIVE MRT AND β_{sys} VALUES

	8-12 μ m FLIR		3-5 μ m FLIR
	1974 Technology	1978-79 Technology	1974 Technology
MRT_0 ($^{\circ}$ K)	0.0254	0.0112	0.0171
β_{sys} (mrad/cycle)	0.996	0.633	1.006
r^2	0.99	0.99	0.99

Equation 6 is the range performance at 50 percent confidence level ($\text{SNR}_N = 1$). To determine range performance at the 10 percent confidence level and the 90 percent confidence level refer to Fig. 3. The value on the normalized curve for a probability of 10 percent is $\text{SNR}_N = 0.5$, and for a probability of 90 percent it is $\text{SNR}_N = 1.5$. Therefore, rewriting Eq. 6, we get

$$R_\rho = \frac{\ln \left(\frac{1}{k_\rho} \frac{\Delta T \sqrt{\epsilon/\gamma}}{\text{MRT}_0} \right)}{\beta_{\text{atm}} + \frac{\gamma}{S} \beta_{\text{sys}}}, \quad (7)$$

where R_ρ is the expected range for probability ρ of detection or recognition and k_ρ is the normalized SNR for probability ρ . When, for example,

$$\begin{aligned} \rho = 0.90, & \quad k_\rho = 1.5; \\ \rho = 0.50, & \quad k_\rho = 1.0; \\ \rho = 0.10, & \quad k_\rho = 0.5. \end{aligned}$$

Validation of Eq. 7 has been shown in Ref. 2.

The next section presents some data that can be used as input to Eq. 7.

III. INPUT DATA

This section contains sample values for the parameters in Eq. 7. These data are inputs that we have used at IDA and represent our best understanding of the problem. These data are only intended to be examples of the inputs necessary to calculate the range for certain probabilities of detection and recognition using the method discussed in this paper.

The sample input values are arranged by type of parameter: FLIR system specifications, task difficulty factors, target specifications, and atmospheric or environmental factors. A discussion is presented wherever it is necessary to comment on the source of the data and on reservations we may have about the accuracy or validity of the models used.

A. FLIR SYSTEM SPECIFICATIONS

<u>Parameter</u>	<u>Description</u>		
MRT_0	y-intercept of the regression line fitted to the values of the MRT in the specifications of the particular FLIR sensor of interest (Fig. 4). This relates to the overall FLIR sensitivity.		
β_{sys}	Slope of the regression line fitted to the values of the MRT in the specifications of the particular FLIR sensor of interest (Fig. 4). This relates to the FLIR resolution.		
<u>Sample Values</u>			
	<u>8-12 μm FLIR</u>		<u>3-5 μm FLIR</u>
	<u>1974</u>	<u>1978-79</u>	<u>1974</u>
MRT_0 ($^{\circ}$ K)	0.0254	0.0112	0.0171
β_{sys} (mrad/cycle)	0.996	0.633	1.006

B. TASK LEVEL FACTORS

<u>Parameter</u>	<u>Description</u>
ϵ	Bar aspect ratio (length-to-width ratio of a single bar) of line pairs placed across a rectangular cross section of the target where width of the rectangle is equal to the minor dimension of the target and length is the major dimension (Fig. 5).
γ	Task level factor, the number of bar chart line pairs per minor dimension of the object.
k_p	Scaling factor for determining range for probability of detection or recognition equal to p .

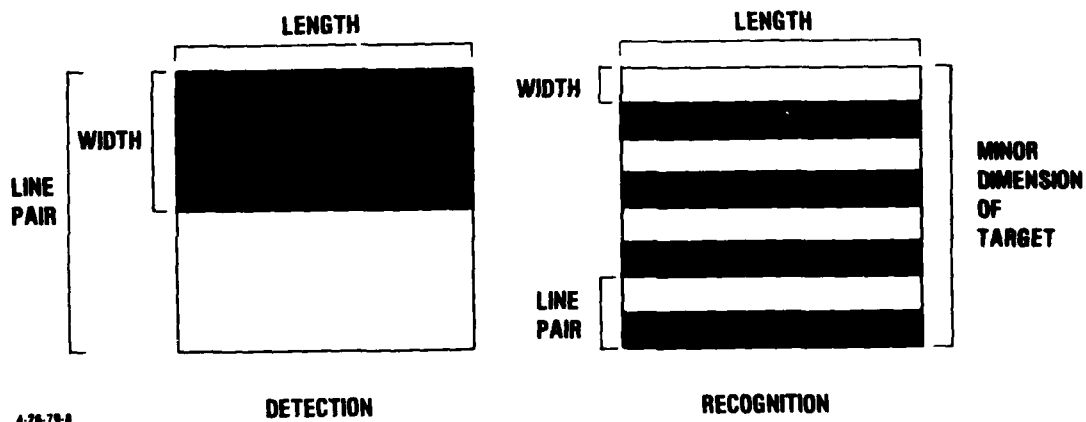


FIGURE 5. Bar test pattern for the front aspect of a tank.

Discussion

Figure 5 shows the bar test pattern used for the front aspect of a tank. For the front aspect of a tank the rectangle is assumed to be approximately square so that the length and

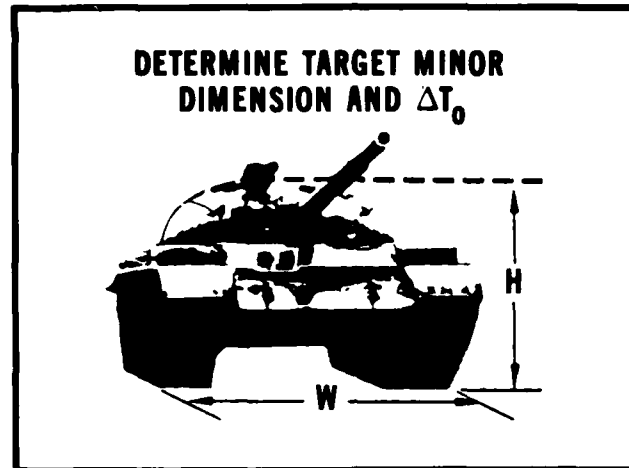
width are both equal to the minor dimension of the tank (the height). However, for the side aspect of a tank the length would be increased, while the width of the rectangle would remain equal to the height of the tank. For our sample values we assume a tank that has length equal to approximately three times its height.

Sample Values

The number of bars placed across the rectangle has been determined to be 2 for detection and 8 for recognition (Ref. 4), as shown in Fig. 5. Examples of aspect ratios are the following:

Rectangle Aspect Ratio	Front Aspect Tank Width=3m Height=3m		Side Aspect Tank Length=9m Height=3m	
	1:1		3:1	
	Detection	Recognition	Detection	Recognition
γ (Number of Line Pairs)	1	4	1	4
Number of Bars	2	8	2	8
Bar Aspect Ratio	2:1	8:1	6:1	24:1
ϵ	2	8	6	24
Normalized SNR for Probability $\rho(k_\rho)$ from Fig. 3:				
$k_{.90}$	1.5	1.5	1.5	1.5
$k_{.50}$	1.0	1.0	1.0	1.0
$k_{.10}$	0.5	0.5	0.5	0.5

C. TARGET SPECIFICATIONS



4-3-79-8

<u>Parameter</u>	<u>Description</u>
S	Target size is the minor dimension of the target expressed in meters.
ΔT	Effective temperature difference (thermal contrast) between the target and the background in degrees Kelvin.

Sample Values for a Tank Target

S	The minor dimension of a tank is its height. Generally we have been using 3 meters as the height of U.S. tanks; therefore S = 3 meters.	
	<u>Front Aspect Tank</u>	<u>Side Aspect Tank</u>
ΔT	$\leq 2^{\circ}K$	$\leq 6^{\circ}K$

D. ATMOSPHERIC FACTORS

<u>Parameter</u>	<u>Description</u>
β_{atm}	Extinction coefficient of the atmosphere (km ⁻¹), which is the sum of the extinctions due to molecular absorption, water vapor continuum, and aerosols:

$$\beta_{\text{atm}} = \beta_{\text{mol}} + \beta_{\text{H}_2\text{O cont}} + \beta_{\text{aer}}$$

Discussion

This atmospheric parameter is complex and requires a brief review in this section. A detailed discussion of the knowledge to date on this subject can be found in Ref. 7, Chapter III, "Atmospheric Effects on Infrared Systems," by J.B. Goodell and R.E. Roberts.

As indicated above, β_{atm} comprises three components: extinction due to molecular absorption, water vapor continuum, and aerosols. For this discussion of extinction Beer's law is assumed ($\tau_{\text{atm}} = e^{-\beta R}$), and therefore transmission through the atmosphere (τ_{atm}) will be calculated. Once τ_{atm} is determined and range R is selected, β can be obtained.

The two components molecular absorption and water vapor continuum are computed in computer code LOWTRAN 3b, developed by the Air Force Geophysics Laboratory to calculate atmospheric transmittances (Ref. 8). This computer code is widely accepted as the best model for computing molecular band absorption. LOWTRAN 3b also calculates the aerosol component, but this will be discussed separately.

The following tables enable the user to obtain a value for the molecular extinction coefficient β , given the atmospheric temperature T_a ($^{\circ}\text{C}$), the dew point T_{dp} ($^{\circ}\text{C}$), and the range R (km). The values of β are derived from the molecular and water vapor continuum components of atmospheric transmission as computed using the LOWTRAN 3b code for a horizontal sea-level path, and a weighting function corresponding to a blackbody source at 10°C .

Table 2 presents extinctions for the 3-5 μm band. Note that atmospheric temperature T_a is not needed in order to find β_{3-5} ; only the dew point T_{dp} and range R are necessary. For a given T_{dp} , a change in T_a does not produce any appreciable difference in β_{3-5} . Therefore, all ranges appear together in one table.

For the 8-12 μm band, both T_a and T_{dp} are needed to find the appropriate β_{8-12} , so a separate table is provided for each range. Tables 3 through 6 correspond to ranges of 2, 4, 8, and 16 km, respectively.

The relationship between τ_{atm} and R assuming Beer's law (Eq. 2) for the 8-12 μm band is not as strong as for the 3-5 μm band. Therefore, the range R to be used in looking up the appropriate $\beta_{mol} + \beta_{H_2O}$ cont in Tables 3 through 6 should be estimated. Using the estimated value of R, the value for extinction is selected, and Eq. 7 is solved for R. If R is somewhat different from the R used to look up the extinction value, Eq. 7 should be solved again using the more appropriate value for extinction. This process is shown in the example presented at the end of the paper.

For values of T_a , T_{dp} , or R other than those given, a linear interpolation scheme between the nearest given values will yield a fairly accurate result.

Again, these values of β account for only the molecular and water vapor continuum components of extinction. To obtain a realistic estimate of detector performance, the aerosol component of extinction must be taken into account as well.

There are many uncertainties regarding aerosol effects on FLIR systems. LOWTRAN 3b contains aerosol models whose validity is in doubt. However, the data given in LOWTRAN 3b are used for our purposes. We have derived approximations based on the LOWTRAN 3b aerosol data. The derivation of these aerosol

TABLE 2. 3-5 μm MOLECULAR PLUS H₂O CONTINUUM EXTINCTION COEFFICIENT FOR TARGET TEMPERATURE OF 10°C

Range (km)	T _{dp} (°C)												
	-20	-15	-10	-5	0	5	10	15	20	25	30	35	40
0.5	.602	.643	.691	.745	.810	.880	.956	1.038	1.128	1.225	1.331	1.439	1.557
1.0	.381	.411	.446	.486	.529	.576	.629	.685	.747	.810	.875	.947	1.024
2.0	.246	.268	.292	.318	.349	.381	.415	.452	.490	.532	.576	.622	.672
4.0	.161	.176	.192	.211	.231	.252	.275	.299	.325	.351	.379	.410	.443
8.0	.107	.117	.129	.141	.154	.168	.183	.199	.215	.233	.252	.275	.300
16.0	.072	.079	.087	.095	.104	.113	.123	.133	.145	.158	.173	.190	.210
32.0	.049	.054	.059	.065	.070	.077	.084	.091	.100	.111	.122	.136	.151

TABLE 3. 8-12 μm MOLECULAR PLUS H₂O CONTINUUM EXTINCTION COEFFICIENT FOR TARGET TEMPERATURE OF 10°C AND PATH LENGTH R=2.0 km

T _a (°C)	T _{dp} (°C)												
	-20	-15	-10	-5	0	5	10	15	20	25	30	35	40
-20	.039												
-15	.039	.047											
-10	.038	.047	.058										
-5	.038	.046	.057	.075									
0	.038	.045	.056	.073	.099								
5	.037	.044	.055	.071	.096	.137							
10	.037	.044	.054	.069	.093	.131	.195						
15	.037	.043	.053	.067	.090	.126	.185	.283					
20	.036	.043	.052	.066	.087	.121	.176	.267	.417				
25	.036	.042	.052	.064	.085	.117	.168	.254	.393	.616			
30	.036	.042	.051	.063	.082	.113	.161	.241	.371	.579	.907		
35	.035	.042	.050	.062	.081	.110	.156	.230	.352	.547	.852	1.323	
40	.035	.041	.050	.062	.079	.107	.150	.205	.334	.516	.805	1.244	1.908

TABLE 4. 8-12 μm MOLECULAR PLUS H₂O CONTINUUM EXTINCTION COEFFICIENT FOR TARGET TEMPERATURE OF 10°C AND PATH LENGTH R=4.0 km

T _a (°C)	T _{dp} (°C)												
	-20	-15	-10	-5	0	5	10	15	20	25	30	35	40
-20	.032												
-15	.031	.041											
-10	.031	.037	.048										
-5	.030	.037	.046	.062									
0	.030	.036	.045	.060	.085								
5	.030	.035	.044	.058	.081	.120							
10	.029	.035	.043	.057	.078	.114	.175						
15	.029	.035	.043	.055	.076	.109	.165	.258					
20	.029	.034	.042	.054	.073	.105	.157	.243	.384				
25	.029	.034	.041	.053	.071	.100	.149	.230	.361	.571			
30	.028	.033	.041	.052	.069	.097	.143	.218	.341	.536	.838		
35	.028	.033	.040	.051	.067	.093	.137	.207	.322	.504	.787	1.21	
40	.028	.033	.040	.050	.066	.091	.131	.197	.305	.476	.744	1.15	1.73

TABLE 5. 8-12 μm MOLECULAR PLUS H₂O CONTINUUM EXTINCTION COEFFICIENT FOR TARGET TEMPERATURE OF 10°C AND PATH LENGTH R=8.0 km

T _a (°C)	T _{dp} (°C)												
	-20	-15	-10	-5	0	5	10	15	20	25	30	35	40
-20	.025												
-15	.025	.031											
-10	.024	.030	.039										
-5	.024	.029	.038	.053									
0	.023	.029	.037	.051	.074								
5	.023	.028	.036	.049	.070	.107							
10	.023	.028	.035	.047	.067	.101	.159						
15	.023	.027	.034	.046	.064	.096	.149	.237					
20	.022	.027	.034	.045	.062	.092	.141	.223	.354				
25	.022	.027	.033	.043	.060	.088	.134	.210	.332	.525			
30	.022	.026	.033	.042	.058	.084	.127	.199	.313	.489	.777		
35	.022	.026	.032	.042	.056	.081	.122	.188	.296	.461	.726	-	
40	.022	.026	.032	.041	.055	.078	.116	.179	.279	.438	.690	-	-

- Denotes infinite extinction

TABLE 6. 8-12 μm MOLECULAR PLUS H_2O CONTINUUM EXTINCTION
 COEFFICIENT FOR TARGET TEMPERATURE OF 10°C AND
 PATH LENGTH $R=16.0$ km

T_a ($^\circ\text{C}$)	T_{dp} ($^\circ\text{C}$)												
	-20	-15	-10	-5	0	5	10	15	20	25	30	35	40
-20	.020												
-15	.019	.025											
-10	.019	.024	.032										
-5	.019	.023	.031	.045									
0	.018	.023	.030	.043	.065								
5	.018	.022	.029	.041	.062	.096							
10	.018	.022	.029	.040	.059	.091	.145						
15	.018	.022	.028	.038	.056	.086	.136	.217					
20	.017	.021	.027	.037	.054	.082	.128	.203	.320				
25	.017	.021	.027	.036	.052	.078	.121	.191	.302	-			
30	.017	.021	.026	.035	.050	.074	.115	.181	.288	.432	-		
35	.017	.020	.026	.034	.048	.071	.110	.172	.271	.432	-	-	
40	.017	.020	.025	.033	.047	.068	.104	.163	.255	.388	-	-	-

- Denotes infinite extinction

model approximations is discussed at length in Ref. 7. In addition to the LOWTRAN 3b aerosol models (maritime, urban and rural) an aerosol model for dry climates has been developed here. Visibility (VIS) in kilometers is the only input value needed to determine β_{aer} by using the approximations (Table 7).

The uncertainties regarding the aerosol models must be emphasized. There are three basic caveats to keep in mind:

1. The visibility required as input to the aerosol models is not a reliable measure. It is very common for two people to get different values when measuring visibility. For a more detailed discussion see Ref. 7.
2. It is unrealistic to expect any simple scaling model will pertain to all atmospheric conditions. For example, the continental model may not be appropriate for all continental atmospheric conditions; for some limited-visibility conditions

over the continent, the maritime model is a better approximation of those conditions.

3. The models in Table 7 are for ground-level paths. For air-to-ground cases significant differences occur due to vertical structure which cannot be predicted by these models.

TABLE 7. EQUATIONS TO APPROXIMATE β_{aer}

Aerosol Model	8-12 μm	3-5 μm
Maritime	$\frac{0.85}{VIS}$	$\frac{2.24}{VIS}$
Rural	$\frac{0.43}{VIS}$	$\frac{0.42}{VIS}$
Urban	$\frac{0.41}{VIS}$	$\frac{0.60}{VIS}$
Dry	$\frac{0.95}{VIS}$	$\frac{1.76}{VIS}$

Thus, β_{atm} may be determined by using the appropriate value obtained from Tables 2-6 ($\beta_{mol} + \beta_{H_2O\ cont}$) and adding it to β_{aer} calculated by using the approximations for different atmospheric conditions given in Table 7.

IV. AN EXAMPLE OF THE CALCULATION PROCEDURE

I. Assume the following problem specifications:

A. FLIR System Specifications for a 1974 Generation 8-12 μm FLIR:

$$\text{MRT}_o = 0.0254 \text{ } ^\circ\text{K}$$

$$\beta_{\text{sys}} = 0.996 \text{ mrad/cycle}$$

B. Task Level Factors for a Front Aspect Tank 3 Meters in Height for Probability of Detection of 50 Percent:

$$\gamma = 1$$

$$\epsilon = 2$$

$$k_p = k_{.50} = 1.0$$

C. Target Specifications:

$$S = 3 \text{ meters}$$

$$\Delta T = 2^\circ\text{K}$$

D. Atmospheric Factors when Visibility = 2 km under Maritime Environment with $T_a = 10^\circ\text{C}$ and $T_{\text{dp}} = 0^\circ\text{C}$

$$1. \beta_{\text{aer}} = \frac{0.85}{\text{VIS}} = \frac{0.85}{2.0 \text{ km}} = 0.425 \text{ km}^{-1}$$

2. Estimate range (R_{est}) to use in looking up appropriate $\beta_{\text{mol}} + \beta_{\text{H}_2\text{O cont}}$ in Tables 2-6:

$$\begin{aligned}
R_{est} &= \frac{\ln\left(\frac{1}{k_p} \frac{\Delta T \sqrt{\epsilon/7}}{MRT_o}\right)}{\beta_{aer} + \frac{Y}{S} \beta_{sys}} \\
&= \frac{\ln\left(\frac{1}{1} \frac{2 \sqrt{2/7}}{0.0254}\right)}{0.425 + \frac{1}{3} (0.996)} \\
&= \frac{3.740}{0.757} \\
&= 4.9
\end{aligned}$$

Thus we will use Table 4 to look up $\beta_{mol} + \beta_{H_2O \text{ cont}}$ since it is for range = 4 km, which is the closest range to 4.9 km in the tables presented in this report. For $T_a = 10^\circ\text{C}$ and $T_{dp} = 0^\circ\text{C}$ and $R = 4 \text{ km}$, we get $\beta_{mol} + \beta_{H_2O \text{ cont}} = 0.78 \text{ km}^{-1}$. Thus, $\beta_{atm} = 0.425 + 0.078 = 0.503 \text{ km}^{-1}$.

(Note: A linear interpolation could be done between values found in Table 4, where range = 4 km, and Table 5, where range = 8 km, to get $\beta_{mol} + \beta_{H_2O \text{ cont}} = 0.076 \text{ km}^{-1}$.)

II. Solve Eq. 7 for all the input values given:

$$\begin{aligned}
R_p &= \frac{\ln\left(\frac{1}{k_p} \frac{\Delta T \sqrt{\epsilon/7}}{MRT_o}\right)}{\beta_{atm} + \frac{Y}{S} \beta_{sys}} \\
R_{.50} &= \frac{\ln\left(\frac{1}{1} \frac{2 \sqrt{2/7}}{0.0254}\right)}{0.503 + \frac{1}{3} (0.996)} \\
&= \frac{3.740}{0.835} \\
&= 4.48
\end{aligned}$$

Thus, the range at 50 percent probability of detection for the given FLIR and under the given atmospheric conditions is 4.5 km.

REFERENCES

1. Institute for Defense Analyses, *Effect of Weather at Hannover, Federal Republic of Germany, on Performance of Electrooptical Imaging Systems: The Calculation Methodology for a FLIR Using a FORTRAN Program*, IDA Note N-842, L.N. Seekamp, August 1977.
- 2.
- 3.
4. J. Johnson, paper presented at Image Intensifier Symposium, Ft. Belvoir, Virginia, 6-9 October 1958.
5. F.A. Rosell and R.H. Willson, "Recent Psychophysical Experiments and the Display Signal-to-Noise Ratio Concept," Chapter 5 in L.M. Biberman, ed., *Perception of Displayed Information*, Plenum Press, New York, 1973, pp. 167-232.
6. R.L. Legault, "Visual Detection Process for Electrooptical Images: Man--The Final Stage of an Electrooptical Imaging System," Chapter 4 in L.M. Biberman and S. Nudelman, eds., *Photoelectronic Imaging Devices, Vol. 1, Physical Processes and Methods of Analysis*, Plenum Press, New York, 1971, pp. 69-86.
7. U.S. Navy Electrooptical Technology Program Office/ Naval Research Laboratory, *The Fundamentals of Thermal Imaging Systems*, EOTPO Report 46/NRL Report 8311, F.A. Rosell and G. Harvey, eds., May 10, 1979.
8. Air Force Geophysics Laboratory, *Atmospheric Transmittance from 0.25 to 28.5 μm : Supplement LOWTRAN 3b (1976)*, J.E.A. Selby, E.P. Shettle, and R.A. McClatchey, November 1976.